



# Improved retrieval of gas abundances from near-infrared solar FTIR spectra measured at the Karlsruhe TCCON station

M. Kiel<sup>1</sup>, D. Wunch<sup>2</sup>, P. O. Wennberg<sup>2</sup>, G. C. Toon<sup>3</sup>, F. Hase<sup>1</sup>, and T. Blumenstock<sup>1</sup>

<sup>1</sup>Institute of Meteorology and Climate Research, Karlsruhe Institute of Technology, Karlsruhe, Germany

<sup>2</sup>Department of Environmental Science and Engineering, California Institute of Technology, Pasadena, CA, USA

<sup>3</sup>Jet Propulsion Laboratory, California Institute of Technology, Pasadena, CA, USA

Correspondence to: M. Kiel (matthaeus.kiel@kit.edu)

Received: 16 October 2015 – Published in Atmos. Meas. Tech. Discuss.: 23 November 2015

Revised: 19 January 2016 – Accepted: 16 February 2016 – Published: 29 February 2016

**Abstract.** We present a modified retrieval strategy for solar absorption spectra recorded by the Karlsruhe Fourier Transform Infrared (FTIR) spectrometer, which is operational within the Total Carbon Column Observing Network (TCCON). In typical TCCON stations, the 3800–11 000 cm<sup>-1</sup> spectral region is measured on a single extended Indium Gallium Arsenide (InGaAs) detector. The Karlsruhe setup instead splits the spectrum across an Indium Antimonide (InSb) and InGaAs detector through the use of a dichroic beam splitter. This permits measurements further into the mid-infrared (MIR) that are of scientific interest, but are not considered TCCON measurements. This optical setup induces, however, larger variations in the continuum level of the solar spectra than the typical TCCON setup. Here we investigate the appropriate treatment of continuum-level variations in the retrieval strategy using the spectra recorded in Karlsruhe. The broad spectral windows used by TCCON require special attention with respect to residual curvature in the spectral fits. To accommodate the unique setup of Karlsruhe, higher-order discrete Legendre polynomial basis functions have been enabled in the TCCON retrieval code to fit the continuum. This improves spectral fits and air-mass dependencies for affected spectral windows. After fitting the continuum curvature, the Karlsruhe greenhouse gas records are in good agreement with other European TCCON data sets.

## 1 Introduction

Global climate change is a major research topic of today's environmental sciences. Human activities, such as burning of fossil fuels, are the key drivers of the continuing increase of atmospheric greenhouse gases and the gases involved in their chemical production (Peters et al., 2013). Long-term measurements of the atmospheric composition provide the experimental data to quantify sinks and sources which are of utmost importance to understand the anthropogenic impact on global warming (Olsen and Randerson, 2004).

The Total Carbon Column Observing Network (TCCON) provides measurements of column-averaged abundances of greenhouse gases. TCCON is a ground-based network of Fourier Transform Infrared (FTIR) spectrometers initiated in 2004 by the California Institute of Technology, Pasadena, USA (Wunch et al., 2011). The stationary high-resolution FTIR spectrometers measure total columns of CO<sub>2</sub>, CO, CH<sub>4</sub>, N<sub>2</sub>O, H<sub>2</sub>O, HF and other atmospheric gases. Precise and accurate column abundances are retrieved from near infrared (NIR) solar absorption spectra using direct sunlight. TCCON measurements are tied to the World Meteorological Organization (WMO) scale via in situ aircraft measurements flown over TCCON sites (Washenfelder et al., 2006; Deutscher et al., 2010; Wunch et al., 2010; Messerschmidt et al., 2011; Geibel et al., 2012). For the greenhouse gases CO<sub>2</sub> and CH<sub>4</sub>, TCCON achieves an accuracy and precision in total column measurements of about 0.2 % which is necessary to gain information about sinks and sources and for satellite validation (Rayner and O'Brien, 2001). Currently, about 23 globally distributed sites are affiliated with TC-

CON. The network aims to improve global carbon cycle studies and to provide a primary validation data record of various gaseous atmospheric components for retrievals from space-based instruments. TCCON instruments measure the same quantities in the same spectral region as satellite-borne instruments – e.g., the Orbiting Carbon Observatory 2 (OCO-2, Frankenberg et al., 2015), the Scanning Imaging Absorption Spectrometer (SCIAMACHY, Frankenberg et al., 2006) and the Greenhouse Gases Observing Satellite (GOSAT, Morino et al., 2011). Hence, for the validation, TCCON provides an ideal data set.

The TCCON strives to attain the best site-to-site precision and accuracy possible. Systematic biases that are consistent throughout the network are fully accounted for by scaling the TCCON retrieval results to the WMO scale via aircraft and AirCore profiles (Wunch et al., 2010). Thus, the TCCON sets guidelines to ensure that the instrumentation at each site is as similar as possible, and that the retrieval software, including the spectroscopic line lists and line shapes, is identical for each site. For example, if a particular site used a different spectroscopic line list from the rest of the sites, the network consistency would decrease even if that line list is an improvement over the original. There are, however, several site-specific differences that can cause a degradation in the TCCON's consistency: differing instrument line shapes (ILS) between instruments (Hase, 2012), laser sampling errors (LSE) that differ between instruments (Messerschmidt et al., 2010), and differing optical component responses between instruments (beam splitters, detectors, filters, mirror coatings, etc.). The impacts of ILS differences are mitigated by requiring that all instruments maintain a near-perfect ILS at each TCCON station. The impacts of the LSE are minimized by applying a correction to the TCCON interferograms (Dohe et al., 2013; Wunch et al., 2015). TCCON partners typically use very similar optical components, and detectors which addresses the last of these issues. This approach to standardizing the optical components is imperfect, but the differences between spectra from different sites are generally small. The Karlsruhe system, however, has a significantly different optical setup, designed to allow for automated mid-infrared NDACC (Kurylo, 1991) and TCCON measurements to be made from the same system. As shown here, using the standard TCCON retrieval approach for this setup causes biases of nearly 1 ppm in  $X_{CO_2}$ , which exceeds the precision requirements of the network.

In this paper, we discuss the particular instrumental setup of the Karlsruhe FTIR spectrometer and point out differences from the standard TCCON setup. We identify difficulties in the standard TCCON data processing when analyzing solar absorption spectra recorded by the Karlsruhe spectrometer and present a strategy for the Karlsruhe data set that improves its consistency with respect to TCCON.

## 2 Instrumentation

The Karlsruhe TCCON FTIR spectrometer was initiated in 2009 at the Karlsruhe Institute of Technology (KIT) – Campus North (49.1° N, 8.4° E, 110 m a.s.l.). Karlsruhe is an extensive urban region in central Europe and experiences an oceanic, mild climate similar to most cities in the mid-western part of Europe. The flat terrain is a favorable scene for nadir-looking satellite overpasses as well as model studies. Solar spectra are acquired by operating a Bruker IFS 125HR spectrometer (Bruker Optics, Germany). The automated instrument is housed in an air-conditioned 20 ft sea transport certified shipping container. The spectrometer features a precise cube-corner Michelson interferometer containing a semi-transparent calcium fluoride ( $CaF_2$ ) beam splitter and a linearly moving scanner. An InSb detector covers the spectral range from 1900–5250  $cm^{-1}$  and an InGaAs detector covers the 5250–11 000  $cm^{-1}$  spectral range. The InSb diode is cryogenically cooled using a liquid nitrogen ( $LN_2$ ) microdosing autofill cooling system (Norhof, Netherlands). A dichroic mirror (Optics Balzers Jena GmbH, Germany) is installed with a cut-on wavenumber of 5250  $cm^{-1}$ . The instrument features a camera-based solar tracker developed by KIT (Gisi et al., 2011) with gold-coated optics to minimize photon noise induced by the visible spectrum. TCCON measurements are routinely recorded at a maximum optical path difference ( $OPD_{max}$ ) of 45 cm leading to a spectral resolution of 0.02  $cm^{-1}$ . In addition, solar spectra are also recorded at  $OPD_{max} = 64$  cm and  $OPD_{max} = 120$  cm leading to spectral resolutions of 0.014 and 0.0075  $cm^{-1}$ , respectively.

### 2.1 Differences to the standard TCCON setup

The Karlsruhe full spectral range is 1900–11 000  $cm^{-1}$ , measured simultaneously with InSb and InGaAs detectors. The typical TCCON spectral range is 3800–16 000  $cm^{-1}$ , measured simultaneously with InGaAs and silicon (Si) detectors (Washenfelder et al., 2006). To measure all TCCON gases, the spectral range of the TCCON measurements must include 3800–11 000  $cm^{-1}$ ; only the oxygen A- and B-bands are measured on the Si detector above 11 000  $cm^{-1}$ , and these retrievals are not part of the standard set of TCCON retrievals (Wunch et al., 2011). The spectra from the Si detector are important, however, because they are used to calculate and correct for any LSE in the system (Wunch et al., 2015), to study aerosols, and the oxygen A- and B-bands are necessary for comparison with satellites, which cannot use the oxygen band at 7885  $cm^{-1}$ .

The Karlsruhe setup splits the 3800–11 000  $cm^{-1}$  spectral range for TCCON-style measurements across the InSb and InGaAs detectors using a dichroic beam splitter that reflects the MIR spectral domain and transmits the NIR spectral range. The cut-on of the dichroic (5250  $cm^{-1}$ ) is between two atmospheric windows separated by  $H_2O$  absorp-

tion bands. In the Earth's atmosphere, this spectral region is strongly saturated such that no loss of information arises by splitting the incoming beam into parts of MIR and NIR radiation at the chosen wavenumber.

For TCCON measurements of CO, N<sub>2</sub>O and HF which absorb in the 3800–4800 cm<sup>-1</sup> region, a narrowband spectral filter transmitting from 3800–5250 cm<sup>-1</sup> is mounted in front of the InSb diode, yielding higher signal-to-noise ratios and minimizing any detector nonlinearity. A spectrum recorded by the Karlsruhe instrument and a typical TCCON spectrum recorded by the Park Falls spectrometer is depicted in Fig. 1.

The operation of the InSb diode provides additional spectral coverage to wavenumbers as low as 1900 cm<sup>-1</sup> when using other narrowband filters. Additional gases absorb in this region, including NO, O<sub>3</sub>, HCl, HCN, C<sub>2</sub>H<sub>2</sub>, C<sub>2</sub>H<sub>4</sub>, NO<sub>2</sub> and C<sub>2</sub>H<sub>6</sub>. Additionally, the fundamental absorption bands of OCS and CO are in this region, making it the preferred spectral region for retrievals of OCS and CO. The optical setup also provides spectra of H<sub>2</sub>O, HDO, CH<sub>4</sub> and N<sub>2</sub>O in the MIR bands. MIR measurements are performed following the guidelines of the Network for the Detection of Atmospheric Composition Change – Infrared Working Group (NDACC-IRWG) in addition to the TCCON measurements in the NIR.

## 2.2 Impact of the optical setup on solar spectra

The combination of the dichroic beam splitter and InSb optical filter in the Karlsruhe FTIR instrument induces stronger variations of the continuum in solar spectra than a standard TCCON FTIR setup. The lower panel of Fig. 1 shows a Karlsruhe spectrum simultaneously recorded by the InSb diode and the InGaAs diode. There are clear differences in the shape of the spectrum between 3900–5250 cm<sup>-1</sup> between the Karlsruhe instrument (Fig. 1, bottom panel) and a typical TCCON instrument (Fig. 1, upper panel). Karlsruhe spectra contain an oscillating overall envelope which is not present in standard TCCON spectra. Retrieved gases within this spectral region are CO (center wavenumber (cw) in cm<sup>-1</sup>: 4233.0, 4290.4), N<sub>2</sub>O (cw: 4395.2, 4430.1, 4719.5), HF (cw: 4038.95) and several H<sub>2</sub>O and HDO narrow spectral windows.

Smaller, but significant differences in the continua are also present in the 5250–11 000 cm<sup>-1</sup> range. The Karlsruhe signal remains high with an oscillating overall envelope while the Park Falls signal decreases smoothly with increasing wavenumbers. This region contains the O<sub>2</sub> (cw: 7885.0) spectral window which is used to calculate column-averaged dry-air mole fractions (DMFs) of the target gases.

## 3 Analysis and data processing

Within TCCON, the recorded interferograms are processed and analyzed with the GGG2014 Software Suite which includes GFIT, a non-linear least-squares spectral fitting algorithm (Wunch et al., 2015). In general, all TCCON sites

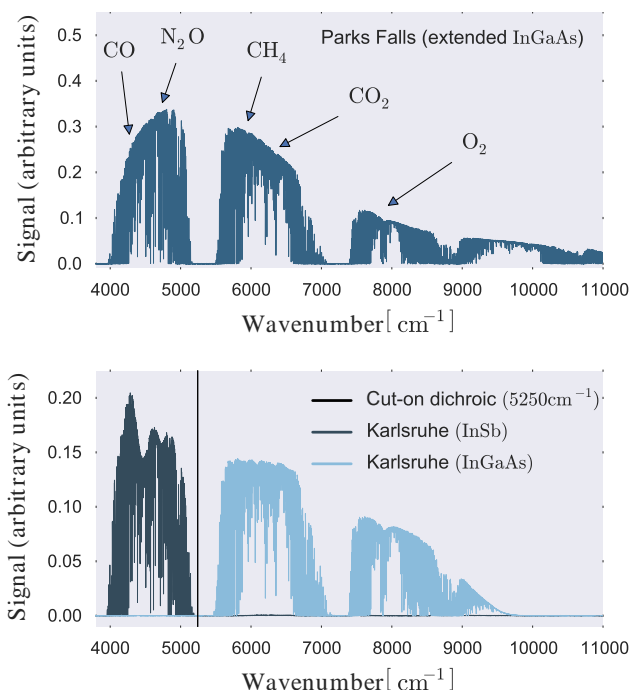


**Figure 1.** Upper panel: typical TCCON spectrum recorded by the Park Falls instrument which operates an extended InGaAs detector, marked are the spectral regions of the main gases of interest; lower panel: typical Karlsruhe spectrum recorded by the InSb and InGaAs diode. The coverage of the full spectral range from 3800–10 000 cm<sup>-1</sup> is realized by the simultaneous operation of the two diodes.

use the same software and retrieval analysis strategy to minimize algorithmic biases between sites. The calibration of the spectral radiances, exact modeling of the far line wing contributions, and continuum transmission variability will cause consistent errors for all TCCON stations, because the line shape and continuum models are identical, thus negligibly impacting the TCCON precision. However, surface temperatures and signal-to-noise ratios can differ significantly from site to site, and therefore these errors are much more important to minimize.

## 3.1 Impact of the optical setup on spectral fits

Ideally, spectral residuals (the difference between the computed and measured spectrum) should have no structure, and consist only of the random noise associated with the signal-to-noise ratio of the measured spectrum. We show that residuals for CH<sub>4</sub> (cw: 5938.0, 6076.0), CO<sub>2</sub> (cw: 6339.5), CO (cw: 4290.4), N<sub>2</sub>O (cw: 4719.5) and O<sub>2</sub> (cw: 7885.0) show significant broad structure when fitted with the standard GGG2014 TCCON retrieval, which fits only a scalar continuum level and linear continuum tilt. Figure 2 shows spectral fits and residuals for one particular Karlsruhe measurement for the O<sub>2</sub> and N<sub>2</sub>O spectral windows. The residuals in the

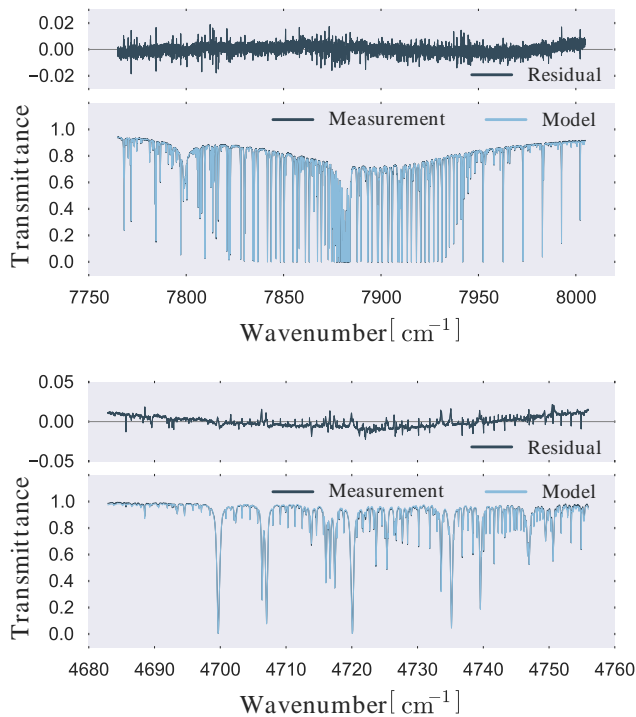


**Figure 2.** Spectral fits for a particular Karlsruhe spectrum: upper panel, spectral fit and residual for O<sub>2</sub> (cw: 7885.0); lower panel, spectral fit and residual for N<sub>2</sub>O (cw: 4719.5).

O<sub>2</sub> spectral window have the shape of a higher-order polynomial while the N<sub>2</sub>O residual has a single extremum. Spectral fits for the other affected target gases and spectral windows are depicted in Fig. A1 in the Appendix.

Continuum curvature is related to our choice of optical filters and dichroic, and is not atmospheric in nature. To demonstrate this, we show that curvature exists in laboratory measurements using a black-body cavity at 1000 °C as a source. The Karlsruhe FTIR instrument is not evacuated, therefore cavity measurements contain some atmospheric absorption lines mainly from H<sub>2</sub>O in the laboratory air (see Fig. A2, Appendix). Nevertheless, the curved residuals from measurements with the black body have a similar shape to residuals of atmospheric measurements. Figure 3 shows spectral fits of the O<sub>2</sub> and N<sub>2</sub>O spectral windows using black-body cavity measurements. For O<sub>2</sub>, residuals follow the shape of a higher-order polynomial as seen for atmospheric measurements (see Fig. 2). Residuals within the N<sub>2</sub>O spectral range follow the same parabolic shape as for atmospheric measurements. This holds for all affected spectral windows (see Fig. A3, Appendix). Hence, curvatures in the residuals are due to the optical setup.

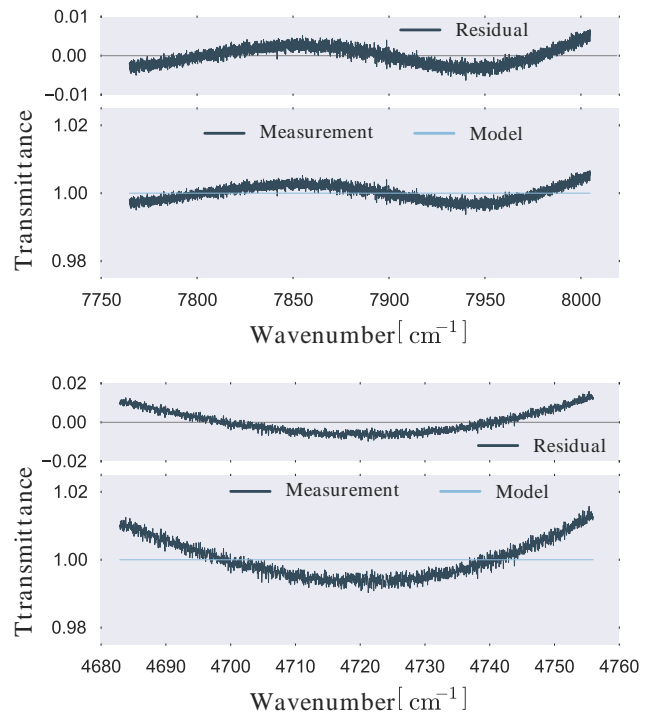


**Figure 3.** Same as Fig. 2 but for Karlsruhe cavity spectra. Both residuals follow the same shape as seen for atmospheric measurements.

#### 4 Fitting in the continuum level

The standard GGG2014 retrieval strategy fits a level and a tilt to the continuum of a spectral window. However, GFIT has also the ability to fit an  $N$ th-order discrete Legendre polynomial basis function to the continuum (Wunch et al., 2015). This continuum fit option is meant to fit curvatures in the continuum of the spectrum that are caused by instrumental features that cannot be neglected in the data processing.

We invoke the higher-order continuum level fit option in GGG2014. We determine the basis function order,  $N$ , for every affected spectral window individually using spectral fits of cavity measurements since their residuals are free from atmospheric absorptions. Different continuum basis function orders are tested to achieve the best fit in the continuum level. An example of how the continuum fit improves residuals of atmospheric spectral fits for the O<sub>2</sub> and N<sub>2</sub>O spectral windows is given in Fig. 4. Spectral fits for all affected target gases are depicted in Fig. A4 in the Appendix.

##### 4.1 Impact of continuum fits on air-mass dependence

Air-mass-dependent retrieval biases must be accounted for, as they can be aliased into the seasonal cycle and affect the time series from different sites at different latitudes differently. There are numerous factors that induce air-mass-dependent artefacts, including continuum curvature.

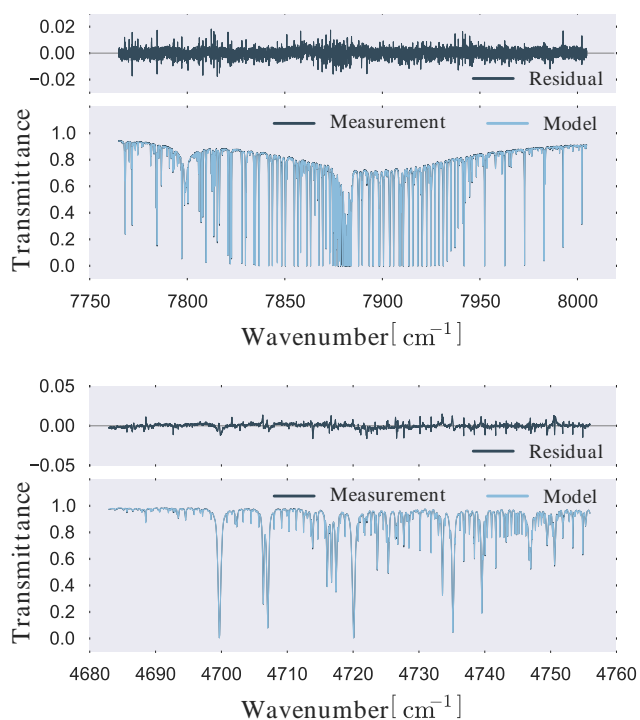


**Figure 4.** Same as Fig. 2 but using the GGG2014 higher-order continuum fit option. For  $O_2$  (upper panel)  $N = 5$  was applied while for  $N_2O$  (lower panel)  $N = 3$  was used.

Using cavity-ratioed spectra as a reference, we show that implementing our continuum curvature fitting scheme significantly reduces the air-mass-dependent biases caused by the curvature. Our cavity-ratioed reference spectra are produced by dividing atmospheric spectra by a high signal-to-noise ratio, reduced-resolution ( $0.05\text{ cm}^{-1}$ ) black-body cavity spectrum ( $1000\text{ }^\circ\text{C}$ ). This ratio eliminates broadband features caused by the optics in the resulting calibrated atmospheric spectra.

The impact of a continuum level fit on the air-mass dependence is elaborated via a case study using Karlsruhe data on 18 May 2014 when high air-mass values up to seven are reached during the measurement day. In Fig. 5, the air-mass dependence compared to the reference retrieval using cavity-ratioed atmospheric spectra is depicted for the  $O_2$  spectral window. Running the standard GGG2014 TCCON retrieval strategy (i.e., fitting only the continuum level and tilt), an overall bias of  $-0.10\%$  results along with an air-mass dependence leading to a relative difference of  $-0.15\%$  between the reference run and the standard TCCON retrieval strategy for air-mass values between six and seven. In comparison, the air-mass dependence for column abundances from the retrieval when a higher-order continuum fit is applied shows neither a significant air-mass dependence nor a significant bias ( $0.04\%$ ).

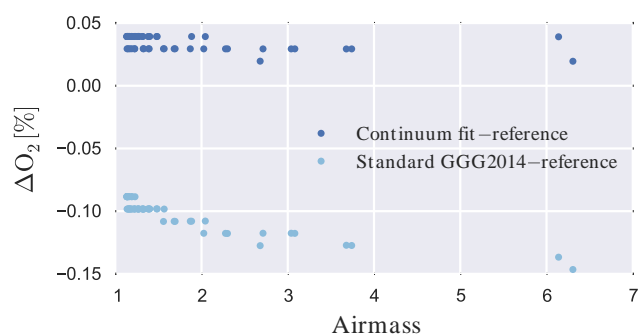


**Figure 5.** Air-mass dependence for the  $O_2$  (cw: 7885.0) spectral window retrieved by the standard GGG2014 TCCON retrieval strategy and using a higher-order continuum fit. As a reference, cavity-ratioed atmospheric spectra are used for the standard GGG2014 retrieval setup.

In general, applying a higher-order Legendre polynomial fit improves the air-mass dependence for  $CO_2$ ,  $CO$ ,  $N_2O$ ,  $O_2$  and  $CH_4$  (cw: 6076.0) (see Fig. A5, Appendix).

There is no clear improvement for  $CH_4$  (cw: 5938.0). On the one hand, the overall bias is reduced for small air-mass values. On the other hand, a stronger air-mass dependence is induced by applying the higher-order continuum level fit. Nevertheless, since the majority of the Karlsruhe measurements are recorded between air-mass values of one and two, the retrieval strategy with a higher-order continuum fit seems to improve the air-mass dependence compared to the standard GGG2014 retrieval. The remaining air-mass dependence is most likely due to spectroscopic errors.

#### 4.2 Impact of continuum fits on column-averaged DMFs

The higher-order continuum fit improves spectral fits as well as the air-mass dependence. It is also important to note that the computed DMFs are changed. DMFs are computed by ratioing the column abundance of the gas of interest by  $O_2$ , and multiplying by the assumed atmospheric DMF of  $O_2$  ( $0.2095$ ). Since  $O_2$  is significantly impacted by continuum curvature, the DMFs of all gases will change compared to the standard GGG2014 retrieval strategy. The relative mean difference is  $(0.132 \pm 0.010)\%$  for the  $O_2$  spectral window. Therefore, DMFs of target gases change by  $0.132\%$  when no higher-order continuum fit is applied in the second retrieval strategy ( $H_2O$ ,  $HF$ , and  $HCl$ ). For all other target gases, any differences are due to the change in retrieved  $O_2$  abundances and changes in abundances retrieved of the target gas itself. An overview of the differences of all affected gases is given in Table 1.

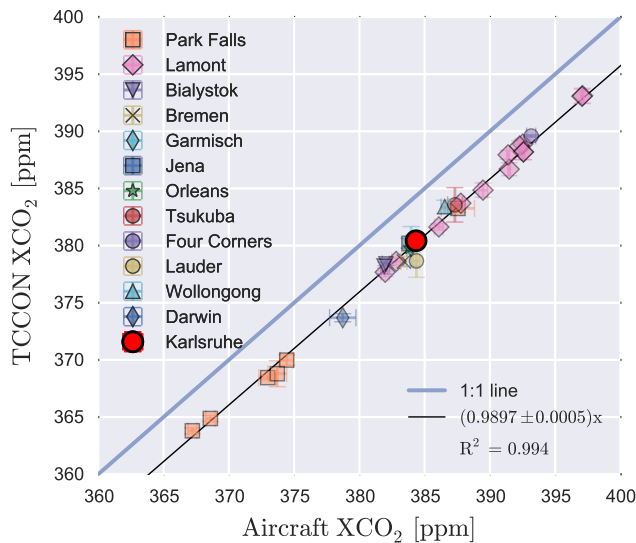


**Figure 6.** Update of the XCO<sub>2</sub> calibration curve which is discussed in detail in, e.g., Wunch et al. (2010), Messerschmidt et al. (2011), and Geibel et al. (2012) using the continuum fit option for the Karlsruhe TCCON data.

## 5 Karlsruhe data in context of other TCCON stations

We compare Karlsruhe TCCON data to aircraft overflights recorded as part of the EU project Infrastructure for Measurement of the European Carbon Cycle (IMECC) in 2009 to provide evidence that the higher-order continuum level fit option improves the consistency of the Karlsruhe data set with other TCCON sites. IMECC was the first airborne campaign to calibrate the European TCCON FTIR sites with respect to the WMO standards.

For our comparison, we rely on IMECC and TCCON data which were presented in detail in, e.g., Wunch et al. (2010), Messerschmidt et al. (2011) and Geibel et al. (2012), where numerous CO<sub>2</sub> in situ profiles were obtained via instruments on an aircraft and compared to CO<sub>2</sub> column amounts from TCCON spectrometers. An update of the calibration curve which has already been discussed in the aforementioned publications with combined results using the IMECC campaign and other aircraft profiles is shown in Fig. 6. The calibration curve contains North American, Australian, Asian and European TCCON sites (see legend within Fig. 6). There is no significant bias between the Karlsruhe data and the aircraft data when comparing the integrated in situ profiles and the Karlsruhe TCCON data (with the higher-order continuum fit option). Karlsruhe data are in good agreement with the other geographically nearby TCCON stations of Orleans (France), Bialystok (Poland), Jena and Garmisch-Partenkirchen (both Germany). Without the higher-order continuum fit, Karlsruhe data is slightly elevated and exhibits an overestimation with respect to the best fit as seen in Fig. 7.

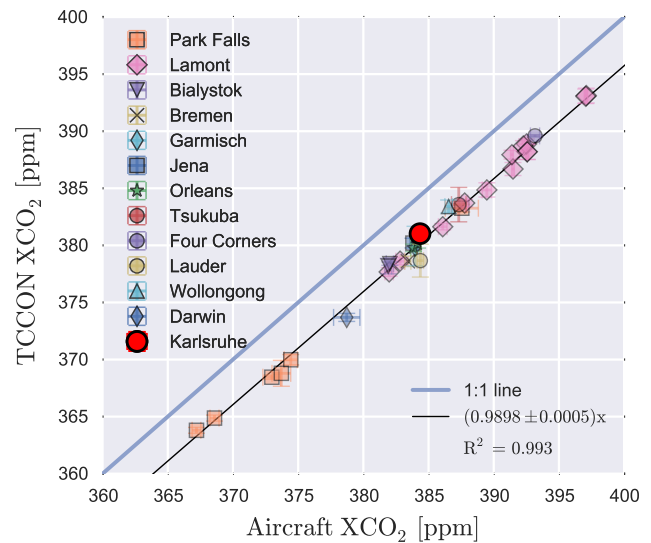


**Figure 7.** Same as Fig. 6 but using the standard GGG2014 TCCON retrieval strategy for Karlsruhe spectra.

In addition, to test how DMFs from other sites are affected when a higher-order continuum fit in the retrieval strategy is applied, we update the calibration curve from, e.g., Wunch et al. (2010), Messerschmidt et al. (2011) and Geibel et al. (2012) using the Karlsruhe retrieval approach to process data of the other TCCON stations which contribute to the TCCON XCO<sub>2</sub> calibration curve (of the particular day of the aircraft overflight).

The differences between XCO<sub>2</sub> retrieved from both retrieval strategies are depicted in Fig. 8. The change in XCO<sub>2</sub> for Karlsruhe is about three times larger than for the other TCCON sites. This shows that a continuum fit to the Karlsruhe spectra is required to improve its consistency with the other TCCON data. The change in XCO<sub>2</sub> is not negligible for the other stations which mainly follow the standard FTIR instrumental setup as recommended by TCCON. However, the changes are consistent (to within 0.1 ppm) for all other TCCON sites, suggesting that the addition of higher-order continuum terms is likely accommodating error that is common across the network. Such error is currently accounted for in scaling to the aircraft/AirCore profiles and thus do not impact the overall accuracy of the TCCON. This suggests that although adding such higher-order terms reduces the site-specific bias at Karlsruhe, it likely has not done so completely. In the next version of the TCCON retrieval software, we will seek to produce a uniform recommendation for modeling the continuum that will accommodate the unique aspects of the Karlsruhe implementation.

## 6 Modified retrieval strategy for Karlsruhe

As seen in the previous sections, the non-standard Karlsruhe data set requires a modification to the standard GGG2014

**Table 1.** Absolute and relative mean differences of retrieved target gases with and without a higher-order continuum fit.

Gas	Abs. mean difference	Standard deviation	Change from O <sub>2</sub>	Rel. mean difference [%]
O <sub>2</sub>	$6.007 \times 10^{21c}$	$0.453 \times 10^{21c}$		$0.132 \pm 0.010$
XAIR	$-1.3 \times 10^{-3}$	$9.8 \times 10^{-5}$	$-1.3 \times 10^{-3}$	$-0.132 \pm 0.048$
XCH <sub>4</sub>	$-2.450^b$	$0.741^b$	$-2.376^b$	$-0.136 \pm 0.041$
XCO <sub>2</sub>	$-0.918^a$	$0.062^a$	$-0.528^a$	$-0.232 \pm 0.016$
XCO	$1.595^a$	$0.490^a$	$-0.132^a$	$2.009 \pm 0.674$
XN <sub>2</sub> O	$-2.203^b$	$0.770^b$	$-0.422^b$	$-0.699 \pm 0.245$

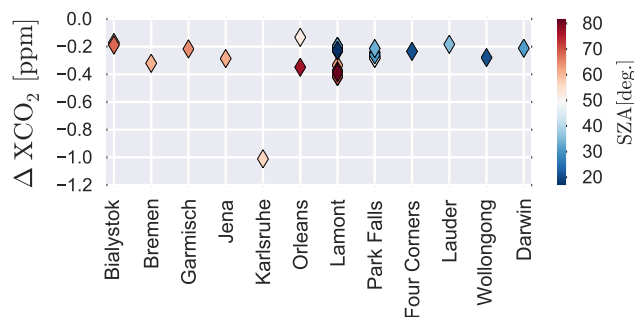
<sup>a</sup> Given in ppm, <sup>b</sup> given in ppb, <sup>c</sup> given in molec cm<sup>-2</sup>.

**Table 2.** Changes for the new Karlsruhe retrieval strategy. Not listed spectral windows will be retrieved by the recommended TCCON retrieval strategy. The three different time periods for the InSb diode correspond to the usage of three different narrowband filters in front of this detector since the instrument was initiated.

Applied <i>N</i> values for Karlsruhe TCCON retrieval					
Affected gases		InGaAs diode		InSb diode	
Gas	Center wavenumber <sup>a</sup>	19 Apr 2010– now	10 Aug 2012– now	22 Nov 2011– 10 Aug 2012	19 Apr 2010– 15 Nov 2011
CH <sub>4</sub>	5938.0	4			
CH <sub>4</sub>	6076.0	5			
CO <sub>2</sub>	6339.5	3			
CO	4233.0		2 <sup>b</sup>	2 <sup>b</sup>	3
CO	4290.4		4	3	4
N <sub>2</sub> O	4395.2		2 <sup>b</sup>	3	3
N <sub>2</sub> O	4430.1		2 <sup>b</sup>	2 <sup>b</sup>	3
N <sub>2</sub> O	4719.5		3	c	c
O <sub>2</sub>	7885.0	5			

<sup>a</sup> Given in cm<sup>-1</sup>, <sup>b</sup> Corresponds to the standard TCCON GGG2014 retrieval strategy where a continuum level and tilt is fitted by default, <sup>c</sup> Not available in this wavenumber region.

TCCON retrieval setup. Instrumental features and the particular optical setup of the Karlsruhe FTIR induce variations of non-atmospheric origin in the recorded solar absorption spectra. The GGG2014 standard retrieval does not take into account continuum curvature in the spectral fitting routine, and thus leads to detrimental curvature in the spectral fits of several spectral windows in the Karlsruhe spectra. Hence, Karlsruhe TCCON data are processed using a higher-order continuum fit for the affected spectral windows by fitting higher-order discrete Legendre polynomial basis functions. We apply three slightly different retrieval approaches for different time periods of the data set because three different narrowband spectral filters were used for the InSb detector since the instrument was initiated in 2009. The different narrowband spectral filters have different optical properties which affect the spectral fits of several spectral windows in a different way. Again, we follow the strategy described in Sect. 4 to determine the polynomial order, *N*, for affected spectral windows for the different filters. An overview of the determined *N* values for filter 1 (used until 15 November 2011) and filter 2 (used until 10 August 2012) is given in Table 2. For

**Figure 8.** Differences in XCO<sub>2</sub> if the Karlsruhe retrieval strategy is applied to data of all TCCON stations which contribute to the XCO<sub>2</sub> aircraft calibration curve. Corresponding solar zenith angles (SZA) of the particular measurement are color coded.

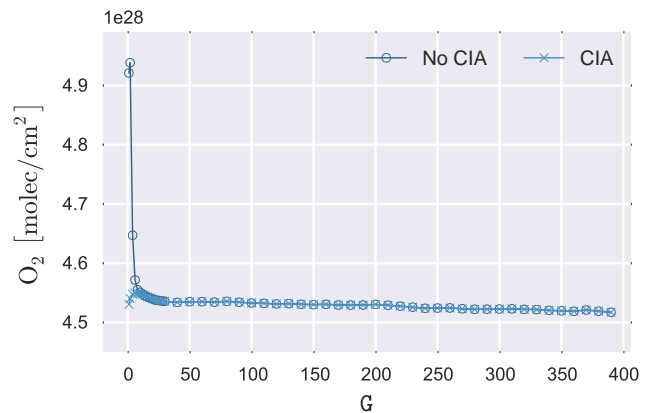
filter 2, one additional spectral window is affected, namely N<sub>2</sub>O (cw: 4395.2) and for filter 1 two more spectral windows are affected, namely CO (cw: 4233.0) and N<sub>2</sub>O (cw: 4330.1).

Table 2 summarizes the modified retrieval strategy for Karlsruhe. Gases which are not listed in Table 2 remain unchanged.

## 7 Spurious air-mass dependence of O<sub>2</sub> retrieval

The results achieved with the modified retrieval setup developed for Karlsruhe in this work indicate that the spurious air-mass dependence of O<sub>2</sub> retrievals is mainly induced by the overlaying collision-induced absorption (CIA). This corroborates earlier studies by Dohe (2013) using PROFFIT (Hase et al., 2004), which also indicated reduced air-mass dependence when using a refined treatment of the background continuum level. The approach includes a fit of the empirical background based on a user-selectable number of baseline points which are evenly distributed across the fitted spectral window. A single point is equivalent to a scaling factor, two points are used to create a linear fit, three or more points create a smooth background, very similar to a cubic spline fit through these guiding points. This choice has been made because each associated derivative is spectrally localized, whereas the fitting of parameters shaping a global polynomial fit across the spectral window results in derivatives which are all strongly interwoven. Dohe demonstrated that a detailed model of the O<sub>2</sub> CIA which overlaps the 1.26  $\mu\text{m}$  absorption band is not required if a sufficiently flexible empirical background fit is included in the fit.

Here, we revisit the O<sub>2</sub> spectral window (cw: 7885.0) and investigate the impact of the number of guiding points,  $G$ , on the retrieved column of molecular oxygen in greater detail using PROFFIT. We expect that a small number of guiding points requires explicit modeling of the CIA, and that a rather flat plateau area is reached for a larger number of guiding points where fits with or without taking CIA into account are essentially equivalent until a further increase finally results in an empirical continuum so flexible that it starts to interact with individual spectral lines, spoiling the retrieved column. The result of this investigation is shown in Fig. 9. Note that the flat plateau area extends at least up to  $G = 400$  – at this value the dimension of the state vector becomes so large that the executable runs out of memory. The retrieved column is slightly decreasing with increasing  $G$ , probably due to the fact that the continuum starts to curve into some broader absorption bands, as the solar H absorption line or the Q-branch of the O<sub>2</sub> band (see Fig. 10). A further improvement of the approach might be achievable by allowing for a variable spacing of guiding points, allowing for a higher degree of flexibility as function of the position in the spectral window. Although the retrieval seems stable for up to the maximum number of guiding points we were able to test, a small number of guiding points is clearly preferable from the technical point of view. In the standard PROFFIT setup for this window  $G = 25$  is used (this setup is currently used for the analysis of low-resolution spectra as recorded with the EM27/SUN, Gisi et al., 2012).



**Figure 9.** Retrieved total column of O<sub>2</sub> with respect to the number of guiding points  $G$  without (no CIA) and with modeling of the collision-induced absorption (CIA).

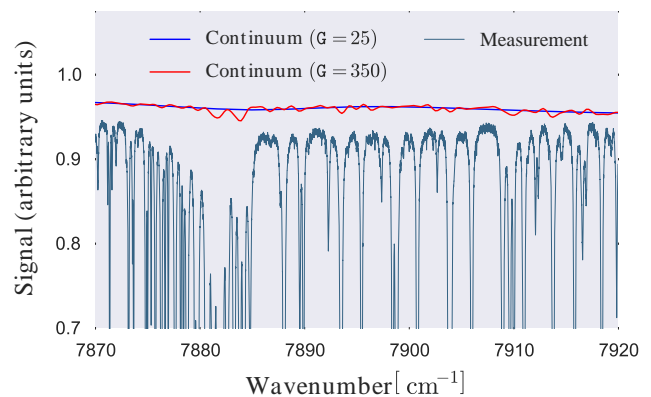


**Figure 10.** Excerpt of the Q-branch in the O<sub>2</sub> spectral window. For  $G = 350$ , the continuum starts to curve into broad solar absorption lines.

Note that the required basis function order empirically determined for the operational TCCON retrieval is smaller (e.g.,  $N = 5$  for the O<sub>2</sub> spectral window) than the number of guiding points required for PROFFIT (larger than 20). This discrepancy might be due to the use of a superior model of the CIA in the GGG2014 Software Suite and due to the fact that the retrieval strategy differs: both algorithms retrieve the O<sub>2</sub> column from the line absorption alone, but GGG2014 in addition allows a scaling of the CIA, whereas PROFFIT only performs a forward calculation of the CIA without any further adjustments of this absorption contribution in the retrieval.

## 8 Implications for NDACC analyses

Whereas the Karlsruhe instrumental setup deviates from the standard TCCON setup, it is quite typical from the NDACC perspective. Several narrow filter bands are defined by use of optical filters in the MIR region covered by the InSb detector. In general, NDACC sites do not use lamp or cavity mea-

surements for correcting a spectral variability of filter transmissions. Traditionally, the analysis of solar absorption spectra using the NDACC methodology relies on narrow spectral fitting regions, typically a couple of tenths up to several wavenumbers wide. The spectral window atlas edited by Meier et al. (2004) provides a comprehensive collection of spectral windows as used for the analysis of MIR spectra. Due to the fact that (1) far line wing contributions emerging from outside the spectral window can only be modeled with limited reliability, (2) the continuum transmission of the atmosphere is variable, and (3) the knowledge of the solar brightness temperature in the spectral region under consideration is limited, an empirical fit of the background continuum is generally included in a retrieval of that window. A single scaling factor is always required – typically a linear slope is also taken into account – and for wider spectral windows encompassing several lines, a second-order polynomial might be appropriate.

The retrieval strategy favored by TCCON prefers much wider spectral fitting regions, which might encompass a whole molecular band of the target gas. This is a superior approach especially in the NIR because using whole absorption bands minimizes any temperature sensitivities, and for a given noise level in the spectrum, this approach significantly reduces the noise error of the retrieved column abundances because many absorption lines contribute. In the future, selection of wider spectral windows might prove useful for NDACC applications as well. From this perspective our

investigation might be useful for future NDACC work also when fits over wider spectral regions are attempted.

## 9 Conclusions

In this work we present a modified retrieval strategy for the Karlsruhe TCCON data set. The Karlsruhe FTIR spectrometer has an extended spectral range and does not conform with the standard TCCON setup. Karlsruhe's particular optical setup induces stronger variations of the spectrum continuum that need to be correctly fitted using a higher-order polynomial fit than provided in the standard GGG2014 Software Suite. Our modified retrieval strategy uses higher-order discrete Legendre polynomial basis functions to fit the continuum which improve spectral fits and air-mass dependencies for affected spectral windows. After this modification, the Karlsruhe data are in good agreement with other European TCCON data sets. A new version (R1) of the Karlsruhe TCCON data is available through CDIAC (<http://tcccon.ornl.gov>). Future scientific studies should use this superior R1 data (Hase et al., 2014), instead of the obsolete R0 data. The setup of the Karlsruhe instrument provides valuable findings for the entire network.

## Appendix A

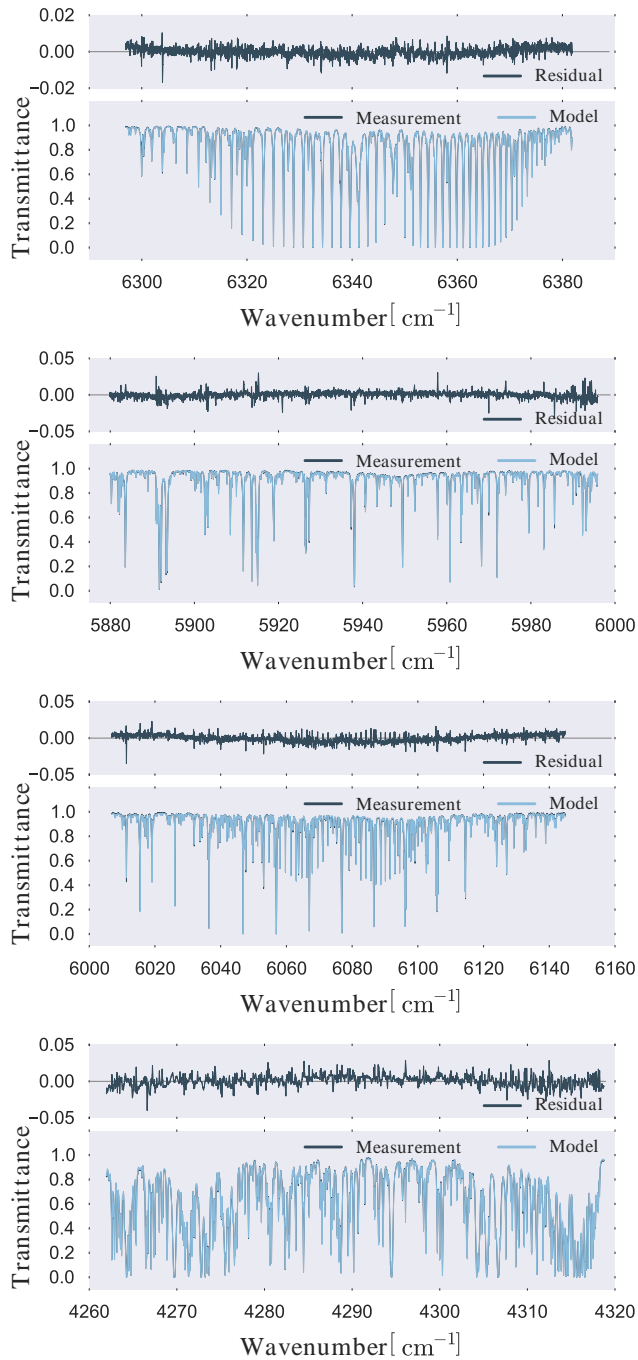


**Figure A1.** Spectral fits for a particular Karlsruhe spectrum: first panel, CO<sub>2</sub> (cw: 6339.5); second panel, CH<sub>4</sub> (cw: 5938.0); third panel, CH<sub>4</sub> (cw: 6076.0); fourth panel, CO (cw: 4290.4). All of the spectral fits show curvature in the residuals.

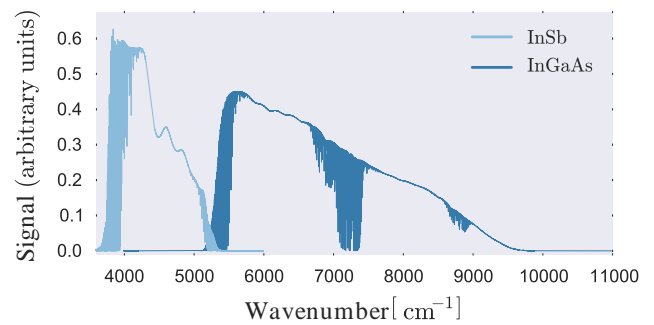


**Figure A2.** Karlsruhe black-body cavity spectra recorded at 1000 °C by the InSb and InGaAs detector.

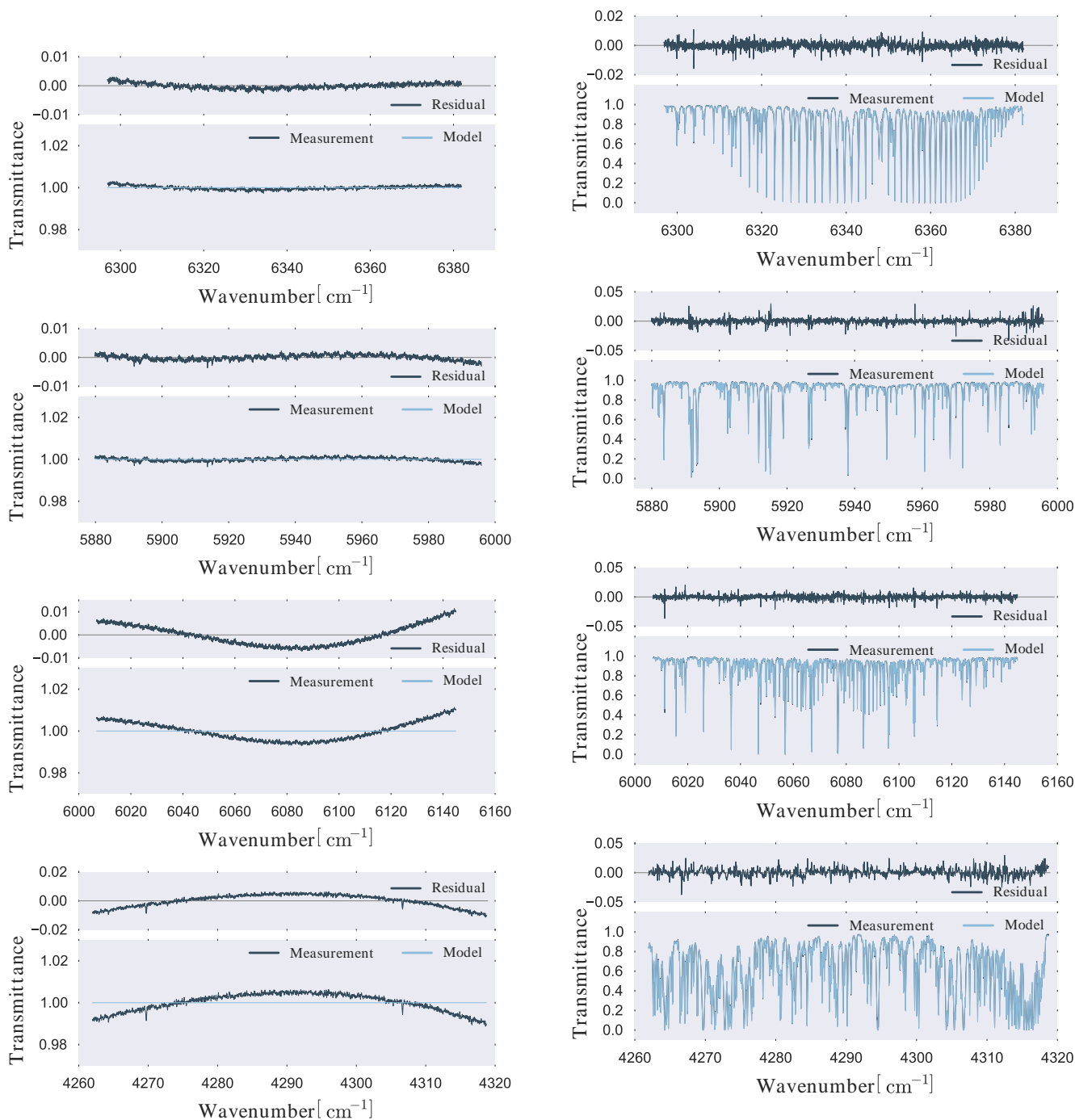


**Figure A3.** Same as Fig. A1 but for Karlsruhe cavity spectra.

**Figure A4.** Same as Fig. A1 but using the GGG2014 higher-order continuum fit option. For CO<sub>2</sub> (first panel)  $N = 3$ , for CH<sub>4</sub> (cw: 5938.0) (second panel)  $N = 4$ , for CH<sub>4</sub> (cw: 6076.0) (third panel)  $N = 5$ , and for CO (fourth panel)  $N = 4$  was applied.

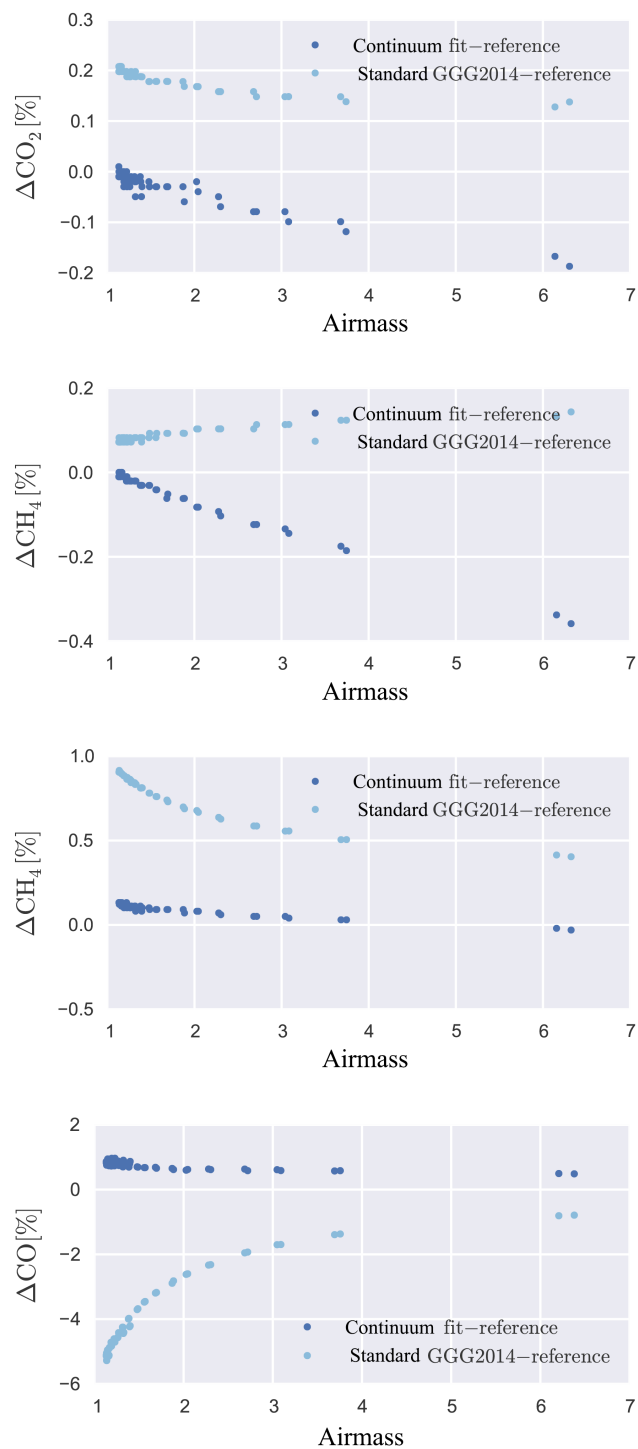


**Figure A5.** Air-mass dependence for the remaining affected spectral windows: first panel,  $\text{CO}_2$  (cw: 6339.5); second panel,  $\text{CH}_4$  (cw: 5938.0); third panel,  $\text{CH}_4$  (cw: 6076.0); fourth panel,  $\text{CO}$  (cw: 4290.4).

*Acknowledgements.* Special thanks are directed to the entire Caltech/JPL Team for making the author's stay at the California Institute of Technology possible. We would like to thank the KIT Graduate School for Climate and Environment (GRACE) for supporting this analysis. This work has been supported by the EU project NORS. We would like to thank NASA for support via grant NNX14AI60G. We acknowledge support by Deutsche Forschungsgemeinschaft and the Open Access Publishing Fund of the Karlsruhe Institute of Technology.

The article processing charges for this open-access publication were covered by a Research Centre of the Helmholtz Association.

Edited by: I. Aben

## References

- Deutscher, N. M., Griffith, D. W. T., Bryant, G. W., Wennberg, P. O., Toon, G. C., Washenfelder, R. A., Keppel-Aleks, G., Wunch, D., Yavin, Y., Allen, N. T., Blavier, J.-F., Jiménez, R., Daube, B. C., Bright, A. V., Matross, D. M., Wofsy, S. C., and Park, S.: Total column CO<sub>2</sub> measurements at Darwin, Australia – site description and calibration against in situ aircraft profiles, *Atmos. Meas. Tech.*, 3, 947–958, doi:10.5194/amt-3-947-2010, 2010.
- Dohe, S.: Measurements of atmospheric CO<sub>2</sub> columns using ground-based FTIR spectra, Dissertation, Karlsruhe Institute of Technology (KIT), Karlsruhe, Germany, 2013.
- Dohe, S., Sherlock, V., Hase, F., Gisi, M., Robinson, J., Sepúlveda, E., Schneider, M., and Blumenstock, T.: A method to correct sampling ghosts in historic near-infrared Fourier transform spectrometer (FTS) measurements, *Atmos. Meas. Tech.*, 6, 1981–1992, doi:10.5194/amt-6-1981-2013, 2013.
- Frankenberg, C., Meirink, J. F., Bergamaschi, P., Goede, A. P. H., Heimann, M., Körner, S., Platt, U., van Weele, M., and Wagner, T.: Satellite cartography of atmospheric methane from SCIAMACHY on board ENVISAT: analysis of the years 2003 and 2004, *J. Geophys. Res.-Atmos.*, 111, D07303, doi:10.1029/2005JD006235, 2006.
- Frankenberg, C., Pollock, R., Lee, R. A. M., Rosenberg, R., Blavier, J.-F., Crisp, D., O'Dell, C. W., Osterman, G. B., Roehl, C., Wennberg, P. O., and Wunch, D.: The Orbiting Carbon Observatory (OCO-2): spectrometer performance evaluation using pre-launch direct sun measurements, *Atmos. Meas. Tech.*, 8, 301–313, doi:10.5194/amt-8-301-2015, 2015.
- Geibel, M. C., Messerschmidt, J., Gerbig, C., Blumenstock, T., Chen, H., Hase, F., Kolle, O., Lavric, J. V., Notholt, J., Palm, M., Rettinger, M., Schmidt, M., Sussmann, R., Warneke, T., and Feist, D. G.: Calibration of column-averaged CH<sub>4</sub> over European TCCON FTS sites with airborne in-situ measurements, *Atmos. Chem. Phys.*, 12, 8763–8775, doi:10.5194/acp-12-8763-2012, 2012.
- Gisi, M., Hase, F., Dohe, S., and Blumenstock, T.: Camtracker: a new camera controlled high precision solar tracker system for FTIR-spectrometers, *Atmos. Meas. Tech.*, 4, 47–54, doi:10.5194/amt-4-47-2011, 2011.
- Gisi, M., Hase, F., Dohe, S., Blumenstock, T., Simon, A., and Keens, A.: XCO<sub>2</sub>-measurements with a tabletop FTS using solar absorption spectroscopy, *Atmos. Meas. Tech.*, 5, 2969–2980, doi:10.5194/amt-5-2969-2012, 2012.
- Hase, F.: Improved instrumental line shape monitoring for the ground-based, high-resolution FTIR spectrometers of the Network for the Detection of Atmospheric Composition Change, *Atmos. Meas. Tech.*, 5, 603–610, doi:10.5194/amt-5-603-2012, 2012.
- Hase, F., Hannigan, J., Coffey, M., Goldman, A., Höpfner, M., Jones, N., Rinsland, C., and Wood, S.: Intercomparison of retrieval codes used for the analysis of high-resolution, ground-based FTIR measurements, *J. Quant. Spectrosc. Ra.*, 87, 25–52, doi:10.1016/j.jqsrt.2003.12.008, 2004.
- Hase, F., Dohe, S., Groß, J., and Kiel, M.: TCCON data from Karlsruhe, Germany, Release GGG2014R1, TCCON data archive, hosted by the Carbon Dioxide Information Analysis Center, Oak Ridge National Laboratory, Oak Ridge, Tennessee, USA, doi:10.14291/tcon.ggg2014.karlsruhe01.R1/1182416, 2014.
- Kurylo, M. J.: Network for the detection of stratospheric change, SPIE Proceedings, *Remote Sens. Atmos. Chem.*, 1491, 168–174, doi:10.1117/12.46658, 1991.
- Meier, A., Toon, G. C., Rinsland, C. P., Goldman, A., and Hase, F.: Spectroscopic Atlas of Atmospheric Microwindows in the Middle Infra-Red, vol. 048 of IRF technical report, Swedish Institute of Space Physics, Kiruna, Sweden, 2004.
- Messerschmidt, J., Macatangay, R., Notholt, J., Petri, C., Warneke, T., and Weinzierl, C.: Side by side measurements of CO<sub>2</sub> by ground-based Fourier transform spectrometry (FTS), *Tellus B*, 62, 749–758, doi:10.1111/j.1600-0889.2010.00491.x, 2010.
- Messerschmidt, J., Geibel, M. C., Blumenstock, T., Chen, H., Deutscher, N. M., Engel, A., Feist, D. G., Gerbig, C., Gisi, M., Hase, F., Katrynski, K., Kolle, O., Lavric, J. V., Notholt, J., Palm, M., Ramonet, M., Rettinger, M., Schmidt, M., Sussmann, R., Toon, G. C., Truong, F., Warneke, T., Wennberg, P. O., Wunch, D., and Xueref-Remy, I.: Calibration of TCCON column-averaged CO<sub>2</sub>: the first aircraft campaign over European TCCON sites, *Atmos. Chem. Phys.*, 11, 10765–10777, doi:10.5194/acp-11-10765-2011, 2011.
- Morino, I., Uchino, O., Inoue, M., Yoshida, Y., Yokota, T., Wennberg, P. O., Toon, G. C., Wunch, D., Roehl, C. M., Notholt, J., Warneke, T., Messerschmidt, J., Griffith, D. W. T., Deutscher, N. M., Sherlock, V., Connor, B., Robinson, J., Sussmann, R., and Rettinger, M.: Preliminary validation of column-averaged volume mixing ratios of carbon dioxide and methane retrieved from GOSAT short-wavelength infrared spectra, *Atmos. Meas. Tech.*, 4, 1061–1076, doi:10.5194/amt-4-1061-2011, 2011.
- Olsen, S. C. and Randerson, J. T.: Differences between surface and column atmospheric CO<sub>2</sub> and implications for carbon cycle research, *J. Geophys. Res.-Atmos.*, 109, D02301, doi:10.1029/2003JD003968, 2004.
- Peters, G. P., Andrew, R. M., Boden, T., Canadell, J. G., Ciais, P., Le Quere, C., Marland, G., Raupach, M. R., and Wilson, C.: The challenge to keep global warming below 2 °C, *Nature Clim. Change*, 3, 4–6, doi:10.1038/nclimate1783, 2013.
- Rayner, P. J. and O'Brien, D. M.: The utility of remotely sensed CO<sub>2</sub> concentration data in surface source inversions, *Geophys. Res. Lett.*, 28, 175–178, doi:10.1029/2000GL011912, 2001.
- Washenfelder, R. A., Toon, G. C., Blavier, J.-F., Yang, Z., Allen, N. T., Wennberg, P. O., Vay, S. A., Matross, D. M., and

- Daube, B. C.: Carbon dioxide column abundances at the Wisconsin Tall Tower site, *J. Geophys. Res.-Atmos.*, 111, D22305, doi:10.1029/2006JD007154, 2006.
- Wunch, D., Toon, G. C., Wennberg, P. O., Wofsy, S. C., Stephens, B. B., Fischer, M. L., Uchino, O., Abshire, J. B., Bernath, P., Biraud, S. C., Blavier, J.-F. L., Boone, C., Bowman, K. P., Browell, E. V., Campos, T., Connor, B. J., Daube, B. C., Deutscher, N. M., Diao, M., Elkins, J. W., Gerbig, C., Gottlieb, E., Griffith, D. W. T., Hurst, D. F., Jiménez, R., Keppel-Aleks, G., Kort, E. A., Macatangay, R., Machida, T., Matsueda, H., Moore, F., Morino, I., Park, S., Robinson, J., Roehl, C. M., Sawa, Y., Sherlock, V., Sweeney, C., Tanaka, T., and Zondlo, M. A.: Calibration of the Total Carbon Column Observing Network using aircraft profile data, *Atmos. Meas. Tech.*, 3, 1351–1362, doi:10.5194/amt-3-1351-2010, 2010.
- Wunch, D., Toon, G. C., Blavier, J.-F. L., Washenfelder, R. A., Notholt, J., Connor, B. J., Griffith, D. W. T., Sherlock, V., and Wennberg, P. O.: The total carbon column observing network, *Philos. T. R. Soc. A*, 369, 2087–2112, doi:10.1098/rsta.2010.0240, 2011.
- Wunch, D., Toon, G. C., Sherlock, V., Deutscher, N. M., Liu, X., Feist, D. G., and Wennberg, P. O.: The Total Carbon Column Observing Network's GGG2014 Data Version, Carbon Dioxide Information Analysis Center, Oak Ridge National Laboratory, Oak Ridge, Tennessee, USA, 43 pp., doi:10.14291/tcccon.ggg2014.documentation.R0/1221662, 2015.